College of Osteopathic Medicine (TUC) Publications and Research

College of Osteopathic Medicine

2018

N-Terminal and Central Domains of APC Function to Regulate Branch Number, Length and Angle in Developing Optic Axonal Arbors in Vivo

Taegun Jin
Touro University California

Gregory Peng
Touro University California

Esther Wu
Touro University California

Shrey Mediratta

Tamira Elul
Touro University California, tamira.elul@tu.edu

Accepted Manuscript

Research report

N-terminal and central domains of APC function to regulate branch number, length and angle in developing optic axonal arbors *in vivo*

Taegun Jin, Gregory Peng, Esther Wu, Shrey Mediratta, Tamira Elul
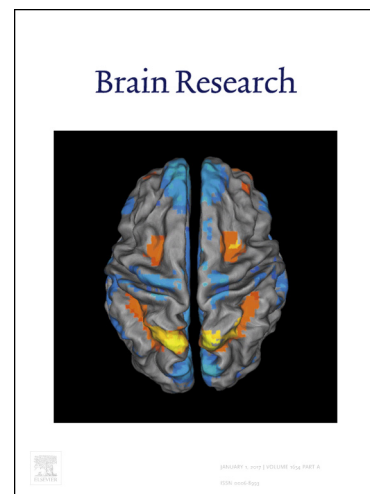
Please cite this article as: T. Jin, G. Peng, E. Wu, S. Mediratta, T. Elul, N-terminal and central domains of APC function to regulate branch number, length and angle in developing optic axonal arbors *in vivo*, *Brain Research* (2018), doi: https://doi.org/10.1016/j.brainres.2018.05.045

N-terminal and central domains of APC function to regulate branch number, length and angle in developing optic axonal arbors *in vivo*

Taegun Jin[1], Gregory Peng[1], Esther Wu[1], Shrey Mediratta[2], and Tamira Elul[1]

[1]Touro University California, Vallejo, California
[2]University of California, Berkeley

Corresponding Author:
Tamira Elul
Department of Basic Sciences
Touro University California
1310 Club Drive
Vallejo, CA 94592

Tel: 707-638-5453   Fax: 707-638-5430   Email: tamira.elul@tu.edu

Running Title: APC shapes optic axonal arbors *in vivo*.

Highlights:
APC is a multifunctional, multidomain protein that modulates microtubule organization as well as ß-catenin stability in the Wnt signaling pathway.

We overexpressed the N-terminal and central domains of APC in individual optic neurons in intact *Xenopus* tadpoles.

Both the N-terminal and central domains of APC decreased numbers and increased lengths of branches in terminal arbors of optic axons *in vivo*.

Overexpression of the N-terminal domain of APC additionally increased bifurcation angle of branches in optic axonal arbors *in vivo*.

However, the APC central domain did not significantly affect branching angle in optic axonal arbors in intact, living tadpoles.

ABSTRACT

During formation of neuronal circuits, axons navigate long distances to reach their target locations in the brain. When axons arrive at their target tissues, in many cases, they extend collateral branches and/or terminal arbors that serve to increase the number of synaptic connections they make with target neurons. Here, we investigated how Adenomatous Polyposis Coli (APC) regulates terminal arborization of optic axons in living *Xenopus laevis* tadpoles. The N-terminal and central domains of APC that regulate the microtubule cytoskeleton and stability of β-catenin in the Wnt pathway, were co-expressed with GFP in individual optic axons, and their terminal arbors were then imaged in tectal midbrains of intact tadpoles. Our data show that the APCNTERM and APCβ-cat domains both decreased the mean number, and increased the mean length, of branches in optic axonal arbors relative to control arbors *in vivo*. Additional analysis demonstrated that expression of the APCNTERM domain increased the average bifurcation angle of branching in optic axonal arbors. However, the APCβ-cat domain did not significantly affect the mean branch angle of arbors in tecta of living tadpoles. These data suggest that APC N-terminal and central domains both modulate number and mean length of branches optic axonal arbors in a compensatory manner, but also define a specific function for the N-terminal domain of APC in regulating branch angle in optic axonal arbors *in vivo*. Our

findings establish novel mechanisms for the multifunctional protein APC in shaping terminal

arbors in the visual circuit of the developing vertebrate brain.

1. INTRODUCTION

Establishment of ordered neuronal connectivity during embryonic development is critical

for proper nervous system function. Accordingly, aberrant development of neural networks is

thought to underlie many neurological and cognitive disorders. The retino-tectal projection of

lower vertebrates, such as tadpoles of the frog *Xenopus laevis*, is an accessible neuronal circuit

that is ideal for studying mechanisms underlying the development of axonal projections *in vivo*.

During formation of the retino-tectal projection, optic axons navigate from the eye to their target

tissue in the brain, the optic tectum. When optic axons invade their target, they elaborate

terminal arbors that make synaptic connections with neurons in specific regions of the tectum

(Alsina et al., 2001; Harris et al., 1987; Sakaguchi and Murphey, 1985). Distinct morphological

features of optic axonal arbors, such as branch number, length, and angle, are important for their

function, potentially influencing the number and pattern of synaptic connections they can make

in the tectum (Alsina et al., 2001; O'Rourke and Fraser, 1990). However, questions remain,

about both the molecular mechanisms that sculpt developing optic axonal arbors *in vivo*, and the

relationships between different branching features in growing optic axonal arbors. In previous

work, we dissected the mechanisms of the Cadherin and Wnt signaling node, β-catenin, in

3

regulating optic axonal arborization in *Xenopus laevis* tadpoles *in vivo* (Wiley et al., 2008; Elul et al., 2003). Here we address how APC, an intracellular signaling molecule in the Wnt pathway that modulates the function of β-catenin, regulates several branching parameters of developing optic axonal arbors *in vivo*.

APC is a large, multi-functional cytoplasmic protein first identified because of its association with hereditary colon cancer, and more recently, implicated in brain cancer and several neurological disorders (Bendelsmith et al., 2018; Azofra et al., 2016; Li et al., 2016; Jaiswal et al., 2005). The molecular mechanisms of APC functions are largely due to its critical role in the Wnt signaling pathway (Senda et al., 2005). In the Wnt signaling pathway, APC functions to modulate levels of ß-catenin. APC normally binds to β-catenin via its central domain. However, following activation of Wnt signaling, APC (along with other factors such as Axin) is uncoupled from β-catenin, which leads to an increase in β-catenin levels in the cytoplasm (Clevers and Nusse, 2012). Canonical Wnt signaling further results in increased β-catenin translocation into the nucleus, where it induces gene transcription together with TCF/LEF factors. In addition to its function in the Wnt signaling pathway, APC is also a microtubule regulator (Senda et al., 2005). In particular, the N-terminal domain of APC is known to affect microtubule organization by binding to the microtubule regulator KAP-3 (Chen et al., 2011; Senda et al., 2005). However, the APC N-terminal domain can also regulate oligomerization of APC, which may, in turn, modulate its activity in the Wnt signaling pathway (Chen et al., 2011; Senda et al., 2005).

A few studies have determined initial functions for APC in development of axonal

4

projections and axon branching in neuronal systems. One paper demonstrated that APC, via modulation of β-catenin stability, regulates the overall projection of optic axons in the developing retino-tectal projection of *Zebrafish* (Paridaen et al., 2009). However, this study did not examine how APC modulation of β-catenin stability affected terminal arborization of individual optic axons in the developing retino-tectal circuit of *Zebrafish*. A second group showed that knockdown of APC in mice led to excessive collateral branches in cortical neurons cultured *in vitro* (Yokota et al., 2009). These researchers further demonstrated that expression of the N-terminal domain of APC that regulates indirect microtubule organization (and APC oligomerization) was responsible for modulating the numbers of branches of cortical neurons in culture (Chen et al., 2011). But, it is not known whether the APC N-terminal domain also regulates the number of branches or additional features of axon arbors in other types of neurons *in vivo*. In other studies, APC has also been shown to control axonal outgrowth and growth cone morphology in several types of neurons through altering microtubule regulation and organization (Purro et al., 2008; Koester et al., 2007; Votin et al., 2005; Zhou et al., 2004).

In this paper, we studied how distinct domains of APC that regulate cytoskeletal organization and β-catenin stability shape individual optic axonal arbors in intact, living *Xenopus* tadpoles. We overexpressed the N-terminal and central domains of APC in individual optic neurons in developing eyebuds of *Xenopus* embryos. We then examined how overexpression of APC N-terminal and central domains modulated the number, length and angle of branches in optic axonal arbors in tecta of *Xenopus laevis* tadpoles. The relationship between the number and mean length of branches in optic axonal arbors expressing the APC domains was also investigated. This work defines shared and specific functions for the N-terminal and central

domains of APC in regulating diverse branching features of optic axonal arbors *in vivo*, and advances our understanding of the mechanisms shaping neuronal circuits in the developing vertebrate brain.

2. RESULTS

2.1 Optic axons that express APCNTERM and APCβ-cat mutants project to tectum

APC is a multifunctional protein that regulates microtubule organization, as well as β-catenin stability in the canonical Wnt pathway. To study how APC modulates neuronal development, we constructed two truncated mutants of APC consisting of distinct domains (Fig. 1A). One mutant consisted of the N-terminal region of APC that mediates indirect microtubule regulation (and oligomerization of APC) (APCNTERM, Fig. 1A; Vleminckx et al.,1997). The second construct was comprised of the APC central domain that binds to, and destabilizes β-catenin (APCβ-cat, Fig. 1A; Vleminckx et al., 1997). Each of these mutants was combined with GFP and lipofected into developing optic neurons in eyebuds of one-day-old *Xenopus laevis* embryos (developmental stage 22). For controls, eyebuds of one-day-old embryos were lipofected with only GFP. Four days later, we imaged optic axons that either expressed GFP (controls), or an APC domain together with GFP (experimentals), in tectal midbrains of intact, living tadpoles (developmental stages 46/47; Fig. 1B).

We first examined whether optic neurons lipofected with the APC mutants were able to project axons to their primary target in the brain - the optic tectum. As shown in the representative images, optic axons overexpressing APCNTERM or APCβ-cat domains indeed arrived at, entered into, and arborized in, the dorsal tectum, as did control GFP expressing axons (Fig. 1B). To quantify these observations, we calculated the percentage of embryos lipofected with GFP, or GFP together with an APC domain, that displayed at least one green fluorescent optic axonal arbor in the optic tectum. We determined that approximately 60% of embryos lipofected with the control plasmid displayed GFP expressing axonal arbors in the tectum (n = 24 embryos lipofected with GFP). Additional analysis showed that ~50% of embryos that were lipofected with GFP together with the APCNTERM domain showed fluorescent optic axons in the tectum (n = 19 embryos lipofected with APCNTERM mutant). Lastly, 70% of embryos lipofected with GFP and APCβ-cat plasmids contained GFP-expressing optic axonal arbors in the tectum (n = 21 embryos lipofected with APCβ-cat domain). Therefore, following lipofection of GFP, and GFP together with APCNTERM or APCβ-cat mutants, in eyebuds of developing embryos, significant percentages of tadpoles displayed optic axonal arbors expressing GFP in the optic tectum. These analyses show that overexpression of the N-terminal and central domains of APC does not inhibit the projection of optic axons from the eye to the tectal midbrain in living tadpoles.

2.2 APC mutants decrease numbers of branches in optic axonal arbors *in vivo*

After optic axons arrive at and proceed to invade the optic tectum, they elaborate terminal arbors that make synaptic connections with target neurons (Alsina et al., 2001; Harris et al.,

1987; Sakaguchi and Murphey, 1985). To determine how APC sculpts these terminal arbors, we examined images of GFP control, GFP-APCNTERM or GFP-APCβ-cat domain expressing optic axonal arbors in tectal midbrains of intact, living tadpoles, and quantified their number of branches (Figs. 1B, 1C; Wiley et al., 2008; Elul et al., 2003).

For baseline data, we first analyzed the number of branches in control optic axonal arbors in intact, living tadpoles at developmental stages 46/47. Control optic axonal arbors were moderately branched, with each arbor containing multiple (primary and secondary) branches (Figs. 1B, 1C). The numbers of branches in GFP expressing arbors ranged between 11 and 19 (Figs. 1B, 1C). On average, control, GFP-expressing arbors in stage 46/47 tadpoles contained ~16 branches (SE = 1.04, n = 12 GFP expressing control optic axonal arbors). These numbers of branches we calculated for control GFP arbors here are consistent with measurements we made on control optic axonal arbors in our earlier studies (Wiley et al., 2008; Elul et al., 2003). In our previous studies, control GFP-expressing optic axonal arbors also contained, on average, ~16 branches in stage 46/47 tadpoles (Wiley et al., 2008; Elul et al., 2003).

We next determined how expression of the APCNTERM domain that contains the indirect microtubule regulatory site of APC modified the branching of optic axonal arbors *in vivo*. Images captured of APCNTERM expressing axonal arbors in tecta of living tadpoles showed that they had fewer branches than control GFP optic axonal arbors in the optic tectum (Figs. 1B, 1C). The number of branches in optic axonal arbors that expressed the APCNTERM mutant ranged between 2 and 13 (Figs. 1B, 1C, 2A, 2D). The mean number of branches in APCNTERM expressing optic axonal arbors was 7 (SE = 0.8, n = 18 APCNTERM mutant

expressing arbors), which was approximately half as many branches as were found in control, GFP-expressing arbors (p < 0.05, Fig. 2A). Therefore, overexpression of the APCNTERM mutant significantly decreased the number of branches in optic axonal arbors *in vivo* (Fig. 2A).

Optic axonal arbors expressing the APCβ-cat mutant had fewer branches than both control arbors and arbors expressing APCNTERM *in vivo* (Fig. 1B). In the representative tracings shown, all three APCβ-cat mutant expressing arbors have fewer branches than the three optic axonal arbors expressing the APCNTERM mutant (Fig. 1C). Quantification showed that optic axonal arbors that expressed the APCβ-cat mutant had a range of 1-12 branches (Figs. 1B, 1C, 2A, 2E). Moreover, almost half of the APCβ-cat expressing arbors that we examined displayed between 1-3 terminal branches (Figs. 1B, 1C, 2E). The mean number of branches in all the APCβ-cat mutant expressing arbors was ~ 4 (SE = 0.6, n = 25 APCβ-cat expressing arbors; Fig. 2A). This mean number of branches we calculated for APCβ-cat expressing arbors was approximately 40% less than the mean number of branches in APCNTERM arbors (p < 0.05), and 75% less than the mean number of branches in control optic axonal arbors (p < 0.05; Fig. 2A).

2.3 APCNTERM and APCβ-cat mutants also decrease total arbor branch length *in vivo*

To further determine how the N-terminal and central domains of APC regulate optic axonal arbors *in vivo*, we examined the total branch length for the control and APC mutant expressing axonal arbors. Using the images captured of optic axonal arbors from intact, living tadpoles lipofected with GFP control, APCNTERM mutant, or APCβ-cat mutant, we calculated

the total arbor branch length (TABL) by summing together the lengths of all the branches in the arbor (Mannit et al., 2009; Elul et al., 2003).

Initial analysis showed that control, GFP-expressing optic axonal arbors in tadpoles at developmental stages 46/47, had an average TABL of 413 μm (SE = 37 μm, n = 12 control GFP expressing arbors). The mean value for total branch length of control optic axonal arbors measured here was close to the mean TABL we calculated for control optic axonal arbors in stage 46/47 *Xenopus laevis* tadpoles in our previous study (Elul et al., 2003). In our earlier report, control, GFP expressing optic axonal arbors had a mean TABL of 385 μm (Elul et al., 2003). The difference between the TABL calculated for control optic axonal arbors in this study and in our previous publication was not significant ($p > 0.05$).

Further measurement showed that expression of each of the APC mutants decreased the total branch length of the terminal arbors of optic axons in the optic tectum. For optic axonal arbors that overexpressed APCNTERM, we calculated a mean TABL of 277 μm (SE = 33 μm, n =16 APCNTERM expressing arbors). This TABL measured for APCNTERM expressing arbors was 37% smaller, and significantly less than, that calculated for control optic axonal arbors ($p < 0.05$, Fig. 2B). For APCβ-cat expressing arbors, the mean TABL was 172 μm (SD = 14 μm, n = 25 APCβ-cat optic axonal arbors), 55% smaller than the TABL measured for control optic axonal arbors ($p < 0.05$, Fig. 2B). These data show that the APCNTERM and APCβ-cat expressing arbors also both have lower total branch length than control optic axonal arbors *in vivo*.

10

2.4 APC mutants increase mean branch length in optic axonal arbors *in vivo*

Thus far, our results show that optic axonal arbors expressing the APCNTERM or APCβ-cat mutants have fewer branches and lower total branch length than control optic axonal arbors (Figs. 2A, 2B). However, the APC mutants decrease the number of branches in optic axonal arbors more severely than they reduce total branch length of the arbors (Figs. 2A, 2B). The percent differences between the mean number of branches in control GFP and APC mutant expressing arbors are greater than the corresponding percent differences between average TABL measured for control and APC mutant arbors (compare Figs. 2A and 2B). One reason this might occur is if APC mutant expressing arbors contain longer individual branches than control GFP optic axonal arbors. To explore this possibility, we examined, and measured the mean length of, individual branches in optic axonal arbors expressing GFP, and GFP together with APCNTERM or APCβ-cat mutants.

This analysis showed that both APC domain expressing arbors had longer individual branches than control GFP expressing optic axonal arbors *in vivo*. In the representative tracings shown, longer branches are present on the optic axonal arbors expressing APCNTERM compared to the control optic axonal arbors (Fig. 1C). In addition, the left two tracings of the APCβ-cat expressing arbor contain longer branches compared to the tracings of optic axonal arbors expressing APCNTERM (Fig. 1C). For control optic axonal arbors, we calculated a mean length of branches of approximately 26 μm (SE = 6.3 μm, n = 11 GFP expressing arbors). However, APCNTERM expressing arbors had a mean length per branch of 37 μm (SE = 3.2 μm, n = 16 APCNTERM optic axonal arbors), which was 42 % greater than the individual branch

length of control optic axonal arbors (p < 0.05; Fig. 2C). Finally, the mean length per branch for

APCβ-cat expressing optic axonal arbors was 44 μm (SE = 1.1 μm, n = 25 APCβ-cat expressing

arbors), ~70% greater than the mean length of branches in control optic axonal arbors (p < 0.05;

Fig. 2C). Therefore, both the APC mutants increased the mean length of branches in optic

axonal arbors relative to control optic axonal arbors, with the APCβ-cat mutant increasing mean

branch length more than the APCNTERM mutant.

These results indicate that the APCNTERM and APCß-cat domains both decrease the

number, and increase the mean length, of branches in optic axonal arbors *in vivo*. To explore this

data on an individual arbor level, we also plotted the number of branches against the mean length

of branches for optic axonal arbors expressing the APCNTERM and APCß-cat domains (Figs.

2D, 2E). These plots showed that there was a negative correlation between the number and the

mean length of branches in both of the APC domain expressing arbors (Figs. 2D, 2E). Each of

these plots of number versus mean length of branches in APC mutant arbors could be fit with

negatively-sloped regression lines (Figs. 2D, 2E). To further specify the relationship between

the mean number and length of branches in the APCNTERM and APCß-cat expressing arbors,

we performed a Spearman's correlation test. This test confirmed that there was a strong negative

correlation between branch number and length in APCNTERM expressing arbors (r = -0.653, n

=15 APCNTERM arbors, p = 0.004), as well as in optic axonal arbors expressing the APCß-cat

domain (r = -0.652, n = 25 APCß-cat arbors, p = 0.0002). This statistical analysis indicates that

both APCNTERM and APCß-cat mutants regulate number and mean length of branches in optic

axonal arbors in an inverse correlated manner.

12

2.5 APC domains decrease size of target regions of optic axonal arbors *in vivo*

These changes in branch number and length we observed in APC mutant expressing optic axonal arbors likely will lead to corresponding alterations in the morphologies of their target areas in the tectum (O'Rourke and Fraser, 1990). Accordingly, we next sought to determine if expression of the APCNTERM and APCβ-cat mutants also modified the sizes of the target regions of optic axonal arbors *in vivo*. The target territories of optic axonal arbors were delimited by applying a convex hull bounding polygon to each arbor (Fig. 3A; see Methods). We then examined and quantified the areas and perimeters of the convex hulls of control, GFP-expressing optic axonal arbors, and arbors expressing the APCNTERM and APCβ-cat domains, *in vivo*.

Before examining target areas of APC domain expressing arbors, we assessed how the convex hull area of GFP expressing, control optic axonal arbors compared to estimates of target area of control optic axonal arbors based on data in a prior study in *Xenopus* tadpoles at similar developmental stages (O'Rourke and Fraser, 1990). From our data, we calculated a mean area of the convex hulls of GFP control expressing arbors of approximately 3,400 μm^2 (SE = 331.9 μm^2, n = 13 GFP control optic axonal arbors). However, multiplying the published mean length (~ 80 μm) with the mean width (~70 μm) of optic axonal arbors (of similar developmental stages) in the previous study gave an estimated area for optic axonal arbors of approximately 5,600 μm^2 (O'Rourke and Fraser, 1990). As expected, our measured area of the convex hull of optic axonal arbors was smaller (~ 35%) than that obtained by multiplying the previously measured length and width of the arbors.

13

Examination of the convex hull morphologies suggested that the areas of both APC domain expressing optic axonal arbors were smaller than those of control optic axonal arbors (Fig. 3A). For APCNTERM expressing optic axonal arbors, we measured an average area of 2,340 μm^2 (SE = 329.4 μm^2, n = 17 APCNTERM arbors), which was ~30% less than the area of the control arbors (p < 0.05; Fig. 4A). For APCß-cat mutant expressing arbors, the mean area of their convex hulls was even smaller, at 1,341 μm^2 (SE = 179.9 μm^2, n = 29 APCß-cat expressing arbors), approximately 60% less than that of control optic axonal arbors (Fig. 4A). The difference between the areas of the APCß-cat arbors and control GFP expressing arbors was significant (p < 0.05), as was the difference between the areas of the APCß-cat arbors and APCNTERM expressing arbors (p < 0.05).   These analyses confirm that both APC mutants significantly decrease the overall area of the target regions of optic axonal arbors *in vivo*, with the APCß-cat mutant decreasing target area more than the APCNTERM mutant.

As a second measure of size of target fields optic axonal arbors, we also compared the perimeters of the convex hulls of GFP control and APC domain expressing axonal arbors. Measurements indicated that the perimeter for GFP optic axonal arbors was, on average, 314 μm (SE = 26.3 μm, n = 13 GFP axonal arbors). However, the mean perimeter for APCNTERM expressing arbors was 227 μm (SE = 12.6 um, n = 17 APCNTERM arbors), which was ~30% less than that of GFP arbors (p < 0.05; Fig. 4B). The mean perimeter for APCß-cat arbors was also approximately 30% smaller than that of controls, at 208 μm (SE = 12.7 μm, n = 29 APCß-cat arbors). The mean perimeter for optic axonal arbors expressing APCß-cat was significantly less than that of GFP, control expressing arbors (p < 0.05; Fig. 4B). This analysis shows that the

14

APCNTERM and APCß-cat mutants both decreased the perimeters of the target areas of optic

axonal arbors *in vivo* by a similar amount.

2.6 APCNTERM expressing optic axonal arbors have increased bifurcation angles

In addition to size, the shapes of the target areas of optic axonal arbors are relevant for

their physiological connectivity in the developing visual system. A previous study showed that

the relative dimensions of optic axonal arbors correlate with their retino-topic mapping in the

tectum of *Xenopus laevis* tadpoles (O'Rourke and Fraser, 1990). Accordingly, we next sought to

determine whether expression of the APCNTERM and APCß-cat domains in optic axonal arbors

altered the shapes of their target areas of *in vivo*. The fact that APCß-cat mutant arbors have

smaller areas than, but similar sized perimeters as, APCNTERM expressing arbors, suggests that

the two APC domains may differentially modulate the shapes of target areas of optic axonal

arbors (Fig. 3A, also compare Figs. 4A and 4B). To further investigate this issue, we observed

and quantified the roundness (circularity) of the convex hulls delimiting the target fields of

control and APC domain expressing arbors.

Observation of the convex hulls of optic axonal arbors suggested that the APC mutant

expressing optic axonal arbors were differentially misshapen relative to control optic axonal

arbors (Fig. 3A). In particular, APCNTERM expressing arbors appeared somewhat more round,

whereas optic axonal arbors that expressed the APCβ-cat mutant looked more elongated, than

control optic axonal arbors (Fig. 3A). To quantitatively assess the morphologies of the target

areas of these optic axonal arbors, we measured the circularity of their convex hulls. Circularity

ranges from zero to one; a perfect circle has a circularity of one, whereas shapes that are more

15

elongated or irregular than a circle have lower circularities. For control optic axonal arbors, we measured an average circularity of 0.49 (SE = 0.06, n = 13 GFP control arbors). However, for APCNTERM expressing arbors, the mean circularity was 0.54 (SE = 0.05, n = 16 APCNTERM expressing arbors), which was 10% greater than that of control, GFP arbors (Fig. 4C). In contrast, the circularity for the convex hulls of APCβ-cat expressing arbors was, on average, 0.39 (SE = 0.03, n =26 APCß-cat expressing arbors), 20% less than that of control arbors (Fig. 4C). Although these differences between circularity of the hulls of APC mutant and control arbors were small (and not statistically significant (p < 0.05)), they did correlate with our observation that the APCNTERM and APCß-cat expressing optic axonal arbors were somewhat more and less round, respectively, than control optic axonal arbors.

These changes in the roundness of the overall target areas of optic axonal arbors expressing the APC domains may result from modifications in the numbers and lengths of branches in the arbors described above. However, the differential alterations in the shapes of the target fields of optic axonal arbors expressing APCNTERM and APCß-cat mutants may additionally reflect changes in other branching features, such as the bifurcation angles. To explore this possibility, we next examined and quantified the average angle of branching in control and APCNTERM and APCß-cat expressing optic axonal arbors (Figs. 3B, 3C, 4D, 4E). Close observation of images of optic axonal arbors suggested that branching angles appeared wider in arbors expressing the APCNTERM domain relative to control, GFP-expressing arbors (Fig. 3C). Quantitative measurements further showed that control optic axonal arbors had a mean branching angle of 68° (SE = 2.7, n = 91 angles in 10 control GFP arbors; also see Patel et al., 2017). However, for APCNTERM optic axonal arbors, we measured an average bifurcation

angle of 75° (SE =2.9, 93 angles in 16 APCNTERM arbors). The mean bifurcation angle for

APCNTERM arbors was 10% greater than the mean branching angle of the control optic axonal

arbors (p < 0.05; Figs. 4D, 4E). In addition, the measured mean branching angle for APCβ-cat

arbors was 65° (SE =2.7, n =104 angles in 18 APCß-cat arbors), which was not significantly

different than the mean branching angle in control, GFP-expressing optic axonal arbors (p >

0.05; Figs. 4D, 4E). This data shows that expression of the APCNTERM mutant also increases

bifurcation angles of branches, whereas the APCß-cat mutant does not significantly alter the

mean branching angles, in optic axonal arbors *in vivo*.

3. DISCUSSION

In this study, we investigated how the multi-domain, multi-function tumor suppressor

protein APC shapes optic axonal arbors in intact, living *Xenopus laevis* tadpoles. We

constructed two domain mutants of APC; one mutant comprised the N-terminal domain of APC

required for oligomerization and indirect microtubule (and actin) regulation, whereas the second

mutant consisted of the central domain of APC that binds to and decreases the stability of β-

catenin (Vleminckx et al., 1997). Optic axonal arbors that expressed the APCNTERM and

APCβ-cat mutants both had significantly fewer and longer individual branches than control optic

axonal arbors. APCNTERM expressing arbors additionally had wider bifurcation angles of

branches than in control arbors. However, APCβ-cat did not significantly affect mean branching

angle in optic axonal arbors *in vivo*. These findings suggest that the N-terminal and central

domains of APC exert both shared and distinct functions in shaping branching in optic axonal

arbors *in vivo*. Because of the low transfection rate of the APC domains in optic neurons (see Methods), the phenotypes we present here likely reflect specific cell autonomous effects of APC domains on optic axonal arborization *in vivo*. Below, we discuss specific molecular interactions mediated by the N-terminal and central domains of APC that could underlie their respective branching phenotypes in developing optic axonal arbors *in vivo*. However, overexpression of these domains of APC in optic neurons may have perturbed some of the branching features in optic axon arbors through a non-specific mechanism, by blocking other functional domains.

3.1 APC N-terminal domain modulates number and angle of arbor branches *in vivo*

Our findings show that overexpression of the N-terminal domain of APC decreased the numbers of branches of terminal arbors of optic axons *in vivo*. In an earlier study, expression of the N-terminal domain of APC also decreased the numbers of collateral branches in axons of cortical neurons (cultured from mice lacking APC) (Chen et al., 2011). Taken together, these findings suggest that the N-terminal domain of APC may inhibit axon branching in different types of neurons in diverse species. Chen and colleagues (2011) further suggested that the N-terminal domain of APC inhibited axon branching in mouse cortical neurons by altering organization of microtubules (that were splayed apart in growth cones of cortical neurons lacking APC). In our system, the N-terminal domain of APC might also regulate branching in optic axonal arbors by modulating the re-organization of microtubule cytoskeleton needed to initiate a new branch (Dent and Kalil, 2001). The N-terminal domain of APC might regulate such microtubule behaviors in arbor branches through binding to KAP-3 and modulation of its' activity (Fig. 1A; Chen et al., 2011; Senda et al., 2005).

We also show that terminal arbors of optic axons expressing the APCNTERM mutant have significantly larger bifurcation angles than control optic axonal arbors. This suggests an additional, novel function for the APC N-terminal domain in regulating branch angle in developing axon arbors *in vivo*. Similar to its' effects on branch number, the N-terminal domain of APC could regulate branch angle in bifurcating daughter branches by altering microtubule dynamics (Weiner et al., 2016). In support of this idea, in an earlier study, the N-terminal domain of APC was shown to regulate direction of growth cone steering in cultured optic neurons through local enhancement of microtubule extension (Koester et al., 2008). Other microtubule regulating factors such as MAP-1B have also been shown to regulate microtubule dynamics that establish orientation of growth cones in developing axons (Bouquet et al., 2004). Therefore, one possibility is that APC functions in conjunction with MAP-1B to regulate microtubule dynamics that establish particular branching angles in terminal optic axonal arbors *in vivo*.

3.2 The central domain of APC regulates number of branches in optic axonal arbors *in vivo*

In this study, we also show that the central domain of APC (APCβ-cat) that binds to and destabilizes β-catenin decreased the number of branches of optic axon arbors *in vivo* (Fig. 1). Previous work demonstrated that the central domain of APC that modulates β-catenin stability shapes the projections of optic axons in the *Zebrafish* retinotectal projection (Paridaen et al., 2009). However, this earlier study did not determine how individual optic axonal arbors in the tectum of *Zebrafish* were altered by APC modulation of β-catenin stability. Therefore, our study

is the first to show that the central domain of APC that regulates β-catenin stability modulates terminal branching of individual optic axons *in vivo*.

Overexpression of the central domain of APC in optic axonal arbors likely modulates numbers of branches of optic axonal arbors by downregulating β-catenin stability (Zhang and Shay, 2017; Paridaen et al., 2009). One possibility is that APC mediated destabilization of β-catenin modulates axon branching by altering TCF gene transcription in the nucleus, as occurs in the canonical Wnt signaling pathway. Indeed, a previous study suggested that β-catenin signals through the Wnt transcription factor, TCF, to regulate the projection of posterior axons in *C. elegans* (Maro et al., 2009). Alternatively, overexpression of the central domain of APC could modulate axon branching by inhibiting β-catenin activity in the Cadherin adhesion pathway (Paridaen et al. 2009; Nelson and Nusse, 1995). In support of this proposal, we previously showed that a mutant of β-catenin that disrupts its binding to α-catenin in the Cadherin adhesion complex also significantly reduced the number of branches in optic axonal arbors *in vivo* (Elul et al., 2003; Wiley et al., 2008). The β-catenin–Cadherin pathway could affect numbers of branches by regulating adhesive interactions and/or actin dynamics required to initiate a new branch in optic axonal arbors (Dent and Kalil, 2001).

3.3 Compensatory regulation of branch number and length in optic axonal arbors *in vivo*

An additional finding of our study is that optic axonal arbors in *Xenopus laevis* tadpoles expressing the APC mutants display an inverse relationship between branch number and length (Miller-Sims and Bottjer, 2012). Optic axonal arbors that express the APC mutants contain fewer branches than control arbors, but the individual branches in APC mutant arbors are longer

20

than those in control optic axonal arbors *in vivo*. Further, optic axonal arbors expressing the APCβ-cat mutant have even fewer and even longer branches than arbors that express the APCNTERM mutant. This compensatory relationship between branch number and length in APC mutant expressing arbors may reflect a competition between branches within individual optic axonal arbors for a growth promoting factor. For example, each optic axonal arbor may have a limited number of post-synaptic connections, or a fixed amount of wirelength, available to them (Wen et al., 2009; Wen and Chklovski, 2008; Cajal, 1899). If so, in very sparsely branched APC mutant expressing arbors, individual branches could make more post-synaptic sites or take up more wirelength than branches could in more highly branched control arbors. The additional synapses made, or wirelength used, by the branches in the APC mutant expressing arbors might then cause them to grow longer than branches in wildtype arbors (Alsina et al., 2001).

In summary, our results suggest novel shared and distinct functions for the APC N-terminal and central domains in regulating branching in optic axonal arbors *in vivo*. Future work will investigate the molecular, cellular and biophysical mechanisms underlying the regulation of branching features in optic axonal arbors by these APC domains. This work extends our understanding of the functions of APC in sculpting individual optic axonal arbors *in vivo*, and may help clarify its involvement in developing neuronal circuits and neurological diseases.

4. EXPERIMENTAL PROCEDURES

21

Xenopus laevis tadpoles:

  Xenopus laevis tadpoles were generated by natural matings of pairs of male and female frogs primed with Human Chorionic Gonadotrophin. Embryos were cultured in a 10% modified Ringer's solution (MMR) and staged according to Nieuwkoop and Faber (1956). All animals and animal experiments were performed at Touro University California and were approved by the Touro University California Institutional Animal Care and use Committee.

DNA plasmids:

  All DNA constructs were cloned into the *Xenopus* expression vectors pCS2+ or pCS2+MT (originally constructed by D. Turner and R. Rupp). pCS2-GFP has been described in our previous publications (Wiley at al., 2008; Elul et al., 2003). We constructed pCS2-MT-APCNTERM by digesting a pCS2-APC-myc *Xenopus* plasmid (obtained from the gene repository Addgene, plasmid number 16686) with NcoI and EcoRI (see Vleminckx et al., 1997). This excised a 3.1kb fragment consisting of the N-terminal region of APC (aa 1- 1934; see APC1 in Velminckx et al., 1997). We then subcloned this fragment corresponding to the N-terminal region of APC into a pCS2-myc plasmid also digested with NcoI and EcoRI. The pCS2-APCβ-cat mutant was constructed by digesting the pCS2-APC-myc plasmid obtained from Addgene with EcoRI. This excised a 2.8 kb region corresponding to the central region of APC that contains both the 15 and 20 aa repeats that bind to β–catenin (aa1034-1973; see APC4 in Vleminckx et al., 1997). This 2.8 kb central region of APC was then cloned into pCS2+ digested with EcoRI to create pCS2-APCβ-cat. Orientation and identity of the APC fragment inserts in pCS2+MT and pCS2+ vectors were confirmed with diagnostic digests and sequencing.

Lipofection:

To express DNA plasmids in small numbers (1-10) of optic neurons in *Xenopus laevis* tadpoles, we injected a DNA-DOTAP lipofection solution (50-200 nl) into both eyebud primordia of one day old embryos, as described previously (Wiley et al., 2008; Elul et al., 2003; Ohnuma et al., 2002; Holt et al., 1990). The plasmids pCS2-APC-NTERM and pCS2-APCβ-cat were mixed with pCS2-GFP at a 1:1 ratio, and then combined with the DOTAP lipofection reagent at a total of 1:3 ratio (Ohnuma et al., 2002; Holt et al., 1990). Previous studies have shown that co-lipofection of two plasmids into eyebuds of developing *Xenopus* embryos will result in their co-expression in single optic neurons at > 90% frequency (Elul et al., 2003; Ohnuma et al., 2002; Holt et al., 1990).

Lipofection was performed at developmental stages that correspond to the end of the wave of optic neuron differentiation (Stages 22-24; Holt et al., 1990). Previous studies showed that optic neurons begin to express the exogenous proteins approximately eight hours after lipofection (Holt et al., 1990). Therefore, optic neurons should not express the APC mutant proteins until after they have terminally differentiated, and the APC mutants should affect neither the differentiation of optic neurons nor the initial outgrowth of their axons from the eye.

Imaging of Optic Axonal Arbors:

Stage 46/47 tadpoles were anesthetized in a 0.02% tricaine solution and placed in an imaging chamber made of silicon on a glass slide and sealed with a cover slip. Imaging was performed with a Nikon Eclipse E800 widefield upright microscope equipped with epifluorescence (Mercury Arc illumination) and a motorized z-stage (Applied Scientific Instrumentation, MFC-2000). Tadpoles were screened at low magnification (Nikon Plan Apo

23

20X /0.75) for GFP expressing optic axonal arbors in the tectum. The screening showed that 30-60% of lipofected tadpoles contained between one to ten GFP expressing optic axons in both tectal hemispheres. Only those animals whose tecta contained between one to three GFP expressing optic axonal arbors were selected for further imaging. These GFP expressing optic axonal arbors that we imaged were located within different medio-lateral regions of the tectal midbrain, thereby eliminating potential spatial bias in parameters of arborization. A z-series of images of control and mutant GFP expressing optic axonal arbors were captured using a 40X air long working distance objective (Nikon Plan Fluor 40X /0.75) with either a Scion Corporation CCD camera (CFW-1312M) controlled by μ-manager software, or a Nikon CCD camera (DS-5M) controlled by Nikon elements software. Typically, 10-20 z-series images at 1.5 μm intervals were captured for each axonal arbor.

Reconstructions of Optic Axonal Arbors:

Only GFP expressing control or mutant optic axon arbors that could be resolved as single, distinct arbors in the tectum were used for reconstructions. Tracings of each arbor were constructed manually using the free hand tool in ImageJ (NIH, Version) or Microsoft Powerpoint (Version 15.31), or using the pencil tool in Adobe Illustrator (Version 21.1). We created an initial tracing of each arbor based on the maximal Z-projection image. However, these tracings were then extensively refined and modified through frequent reference to the original z-series (z-stack) of images of the arbor (Fig. 1C; also see Lom and Cohen-Cory, 1999). Once we had created the most accurate tracings (reconstructions) of the arbors we could *with respect to the z-series of images of the arbor*, all measurements were then made on these tracings.

Morphometric Measurements:

24

Numbers of branches

To quantify the number of branches per arbor, individual branch tips were manually counted on maximum projections of z-series images captured of optic axonal arbors *in vivo*.

Total Arbor Branch Length

To measure total arbor branch length, we measured all the branches in the arbor and summed their lengths using the freehand line tool on Image J. We first traced and measured the longest, central branch in the arbor. The second and higher order branches of the arbor were also traced and measured using the freehand line tool. Once the measurements were complete, primary, secondary and higher order branch lengths were added to compute the total arbor branch length for each arbor. In our previous study, we used a similar protocol to measure total arbor length but we used the straight line tool rather than the freehand line tool in Image J (Elul et al., 2003). This may explain why our measurements for TABL in this study are slightly larger than those obtained in our previous report (Elul et al., 2003).

Mean Branch Length

We also calculated mean length of individual branches in an optic axonal arbor. Mean branch length was calculated by dividing the total arbor branch length for an arbor by the number of branches in the arbor.

Target Regions of Optic Axonal Arbors *in vivo*

To delimit the target region of an optic axonal arbor, we connected the distal branch tips of the arbor using the polygon tool in Image J to generate a convex hull (red dashed outline of

right most GFP arbor, Fig. 3A; also see Schmidt et al., 2000). The area and perimeter

circumscribed by these convex hull polygons of optic axonal arbors were then determined using

Image J measurement functions (Figs. 4A, B). Circularity of the convex hulls was calculated in

Excel using the formula $C = 4*\pi*Area /(Perimeter)^2$ (Fig. 4C).

Bifiurcation Angles of Branches

To measure bifurcation angles of branching in optic axonal arbors, we first labelled the

longest branch as "primary branch", and the branches that budded from the primary as

"secondary branches". The reference point for the measurement of branching angles was where

primary branch and secondary branch converge. The direction of the angle was determined by

the direction of the projection of the primary optic axon arbor branch, which generally followed

a medio-posterior directed vector (Fig. 3B).

Statistical Analysis:

Quantitative measurements were performed blind to the condition (i.e. construct

expressed) to ensure unbiased assessments of phenotypes. We used the Students' t-test (two-

tailed, unequal variances) to determine statistical significance of difference. $p < 0.05$ was

considered to indicate statistical significance of difference. Excel software was used to store

quantitative measurements, as well as to perform statistical analyses and generate plots.

ACKNOWLEDGEMENTS

We thank Anokh Sohal, Joseph Pinnizzotto and Jacob Galdes for technical help with this project, and Dr. Laura Borodinsky for help with microscopy.

REFERENCES

Alsina B, Vu T, Cohen-Cory S. 2001. Visualizing synapse formation in arborizing optic axons in vivo: dynamics and modulation by BDNF. Nat Neurosci. Nov;4(11):1093-101.

Azofra AS, Kidambi TD, Jeremy RJ, Conrad P, Blanco A, Myers M, Barkovich J, Terdiman JP. 2016. Differences in neuropsychological and behavioral parameters and brain structure in patients with familial adenomatous polyposis: a sibling-paired study. Hered Cancer Clin Pract. Oct 10;14:20.

Bendelsmith CR, Skrypek MM, Patel SR, Pond DA, Linabery AM, Bendel AE. 2018. Multiple pilomatrixomas in a survivor of WNT-activated medulloblastoma leading to the discovery of a germline APC mutation and the diagnosis of familial adenomatous polyposis. Pediatr Blood Cancer. Jan;65(1).

Bouquet C, Soares S, von Boxberg Y, Ravaille-Veron M, Propst F, Nothias F. 2004. Microtubule-associated protein 1B controls directionality of growth cone migration and axonal branching in regeneration of adult dorsal root ganglia neurons. J Neurosci. Aug 11;24(32):7204-13.

Cajal SR. Textura del Sistema Nervioso del Hombre y de los Vertebrados (Texture of the Nervous System of Man and the Vertebrates). 1899. New York: Springer-Verlag.

Chen Y, Tian X, Kim WY, Snider WD. 2011. Adenomatous polyposis coli regulates axon arborization and cytoskeleton organization via its N-terminus. PLoS One. 6(9):e24335.

Clevers H, Nusse R. 2012. Wnt/β-catenin signaling and disease. Cell. Jun 8;149(6):1192-205.

Dent EW, Kalil K. 2001. Axon branching requires interactions between dynamic microtubules and actin filaments. J Neurosci. Dec 15;21(24):9757-69.

Elul TM, Kimes NE, Kohwi M, Reichardt LF. 2003. N- and C-terminal domains of beta-catenin, respectively, are required to initiate and shape axon arbors of retinal ganglion cells in vivo. J Neurosci. Jul 23;23(16):6567-75. Erratum in: J Neurosci. 2003 Sep 17;23(24):0a.

Harris WA, Holt CE, Bonhoeffer F. 1987. Retinal axons with and without their somata, growing to and arborizing in the tectum of *Xenopus* embryos: a time-lapse video study of single fibres in vivo. Development. Sep;101(1):123-33.

Holt CE, Garlick N, Cornel E. 1990. Lipofection of cDNAs in the embryonic vertebrate central nervous system. Neuron. Feb;4(2):203-14.

Jaiswal AS, Balusu R, Narayan S. 2005. Involvement of adenomatous polyposis coli in colorectal tumorigenesis. Front Biosci. May 1;10:1118-34. Review.

Koester MP, Müller O, Pollerberg GE. 2007. Adenomatous polyposis coli is differentially distributed in growth cones and modulates their steering. J Neurosci. Nov 14;27(46):12590-600.

Li D, Wang Z, Chen Z, Lin L, Wang Y, Sailike D, Luo K, Du G, Xiang X, Jiafu GD. 2016. MicroRNA-106a-5p facilitates human glioblastoma cell proliferation and invasion by targeting adenomatosis polyposis coli protein. Biochem Biophys Res Commun. Dec 9;481(3-4):245-250.

Lom B, Cohen-Cory S. 1999. Brain-derived neurotrophic factor differentially regulates retinal ganglion cell dendritic and axonal arborization in vivo. J Neurosci. Nov 15;19(22):9928-38.

Manitt C, Nikolakopoulou AM, Almario DR, Nguyen SA, Cohen-Cory S. 2009. Netrin participates in the development of retinotectal synaptic connectivity by modulating axon arborization and synapse formation in the developing brain. J Neurosci. Sep 9;29(36):11065-77.

Maro GS, Klassen MP, Shen K. 2009. A beta-catenin-dependent Wnt pathway mediates anteroposterior axon guidance in C. elegans motor neurons. PLoS One. 4(3):e4690.

Miller-Sims VC, Bottjer SW. 2012. Auditory experience refines cortico-basal ganglia inputs to motor cortex via remapping of single axons during vocal learning in zebra finches. J Neurophysiol. Feb;107(4):1142-56.

Nelson WJ, Nusse R. 2004. Convergence of Wnt, beta-catenin, and cadherin pathways. Science 303:1483–1487.

O'Rourke NA, Fraser SE. 1990. Dynamic changes in optic fiber terminal arbors lead to retinotopic map formation: an in vivo confocal microscopic study. Neuron. 1990 Aug;5(2):159-71.

Patel A, Bains A, Millet R, Elul T. 2017. Visualizing morphogenesis using the Processing programming language. Journal of Biocommunication. 41(1): 15-21.

Nieuwkoop PD, Faber J. 1956. *Normal table of Xenopus laevis*. Amsterdam: Daudin.

Ohnuma S, Mann F, Boy S, Perron M, Harris WA. 2002. Lipofection strategy for the study of *Xenopus* retinal development. Methods. 28(4):411-9.

Paridaen JT, Danesin C, Elas AT, van de Water S, Houart C, Zivkovic D. 2009. Apc1-mediated antagonism of Wnt/beta-catenin signaling is required for retino-tectal pathfinding in the zebrafish. Zebrafish. Mar;6(1):41-7.

Purro SA, Ciani L, Hoyos-Flight M, Stamatakou E, Siomou E, Salinas PC. 2008. Wnt regulates axon behavior through changes in microtubule growth directionality: a new role for adenomatous polyposis coli. J Neurosci. Aug 20;28(34):8644-54.

Sakaguchi DS, Murphey RK. 1985. Map formation in the developing *Xenopus* retinotectal system: an examination of ganglion cell terminal arborizations. J Neurosci. Dec;5(12):3228-45.

Sanchez AL, Matthews BJ, Meynard MM, Hu B, Javed S, Cohen Cory S. 2006. BDNF increases synapse density in dendrites of developing tectal neurons *in vivo*. Development. Jul;133(13):2477-86. Epub 2006 May 25.

Schmidt JT, Buzzard M, Borress R. 2000. Dhillon S. MK801 increases retinotectal arbor size in developing zebrafish without affecting kinetics of branch elimination and addition. J Neurobiol. Feb 15;42(3):303-14.

Senda T, Shimomura A, Iizuka-Kogo A. 2005. Adenomatous polyposis coli (Apc) tumor suppressor gene as a multifunctional gene. Anat Sci Int. Sep;80(3):121-31.

Vleminckx K, Wong E, Guger K, Rubinfeld B, Polakis P, Gumbiner BM. 1997. Adenomatous polyposis coli tumor suppressor protein has signaling activity in Xenopus laevis embryos resulting in the induction of an ectopic dorsoanterior axis. J Cell Biol. Jan 27;136(2):411-20.

Votin V, Nelson WJ, Barth AI. 2005. Neurite outgrowth involves adenomatous polyposis coli protein and beta-catenin. J Cell Sci. Dec 15;118(Pt 24):5699-708.

Weiner AT, Lanz MC, Goetschius DJ, Hancock WO, Rolls MM. 2016. Kinesin-2 and Apc function at dendrite branch points to resolve microtubule collisions. Cytoskeleton (Hoboken). Jan;73(1):35-44.

Wen Q, Stepanyants A, Elston GN, Grosberg AY, Chklovskii DB. 2009. Maximization of the connectivity repertoire as a statistical principle governing the shapes of dendritic arbors. Proc Natl Acad Sci U S A. Jul 28;106(30):12536-41.

Wen Q, Chklovskii DB. 2008. A cost-benefit analysis of neuronal morphology. J Neurophysiol. May;99(5):2320-8.

Wiley A, Edalat K, Chiang P, Mora M, Mirro K, Lee M, Muhr H, Elul T. 2008. GSK-3beta and alpha-catenin binding regions of beta-catenin exert opposing effects on the terminal ventral optic axonal projection. Dev Dyn. 237(5):1434-41.

Yokota Y, Kim WY, Chen Y, Wang X, Stanco A, Komuro Y, Snider W, Anton ES. 2009. The adenomatous polyposis coli protein is an essential regulator of radial glial polarity and construction of the cerebral cortex. Neuron. Jan 15;61(1):42-56.

Zhang L, Shay JW. 2017. Multiple Roles of APC and its Therapeutic Implications in Colorectal Cancer. J Natl Cancer Inst. Aug 1;109(8).

Zhou FQ, Zhou J, Dedhar S, Wu YH, Snider WD. 2004. NGF-induced axon growth is mediated by localized inactivation of GSK-3beta and functions of the microtubule plus end binding protein APC. Neuron. 2004 Jun 24;42(6):897-912.

FIGURE LEGENDS

Figure 1: APC N-terminal and central domains alter branching in optic axonal arbors *in vivo*.

We constructed truncated mutants consisting of the N-terminal and central domains of *Xenopus laevis* APC (A). The APCNTERM mutant consisted of the N-terminal region of APC (amino acids 1-1034) containing the oligomerization domain and armadillo repeats of APC (A). The APCβ-cat mutant contained the middle third of APC (amino acids 1034-1984) containing the β-catenin binding site of full length APC (A). Example images (B) and reconstructions (C) of optic axonal arbors expressing GFP (controls) or GFP together with an APC mutant (experimentals) in tectal midbrains of intact, living tadpoles (stages 46/47) show alterations in optic axon branching induced by expression of the APC domains. The left most tracing of each group of arbors (C) is based on the arbor image shown in (B). Scale Bar – 30 μm (B); 40 μm (C).

Figure 2: Quantification of effects of APC domains on optic axonal arbors *in vivo*.

Plots of number of branches (A), total arbor branch length (B), and mean branch length (C) confirm observed differences between optic axonal arbors expressing GFP or GFP together with an APC mutant. Data in A-C is shown as percent of control mean with SEM. * above data bar indicates $p < 0.05$ for control versus APC mutant. * above horizontal line indicates $p < 0.05$ for APCNTERM versus APCß-cat condition. Additional scatter plots of number of branches versus mean branch length with regression lines show inverse correlation between these parameters in optic axonal arbors expressing APC domains (D, E).

Sample numbers: A) GFP-12, APCNTERM–18 APCβ-cat-25;

B) GFP-12, APCNTERM-16, APCβ-cat-25; C) GFP-11, APCNTERM-16, APCβ-cat-25

34

Figure 3: APC domains alter target region morphologies and branch angles of optic axonal arbors.

Representative convex bounding polygons outlining control and APC-mutant expressing optic axonal arbors *in vivo* depict differences in overall morphologies of the control and APC domain expressing arbors (A). Illustration of how made measurements of bifurcation angles on a schematic optic axonal arbor (B). Zoomed in regions of images of optic axonal arbors expressing GFP, or GFP with APC domains (left) and tracings of these images (right) show how APC domains alter bifurcation angle (C).

Scale Bar- A) 40 μm; C) 10 μm.

Figure 4: Quantification of morphology and bifurcation angle of optic axonal arbors *in vivo*

Quantification of size (A, B) and shape (C) of convex hull polygons confirm additional differences between morphologies of control and APC mutant expressing optic axonal arbors *in vivo*. Plot and histogram of measurements of mean branch angle in control and APC mutant expressing optic axonal arbors also show alterations in bifurcation angles (D, E).

Data in A-D are presented as percent of control mean with SEM. * above data bar indicates $p < 0.05$ in comparison between control and APC mutant arbors. * above horizontal line indicates p < 0.05 in comparison between APCNTERM and APCß-cat arbors.

Sample Numbers: A-C) GFP-13 arbors, APCNTERM-17 arbors, APCβ-cat-29 arbors; D, E) GFP - 92 angles in 10 arbors, APCNTERM - 93 angles in 16 arbors, APCβcat - 104 angles in 18 arbors.
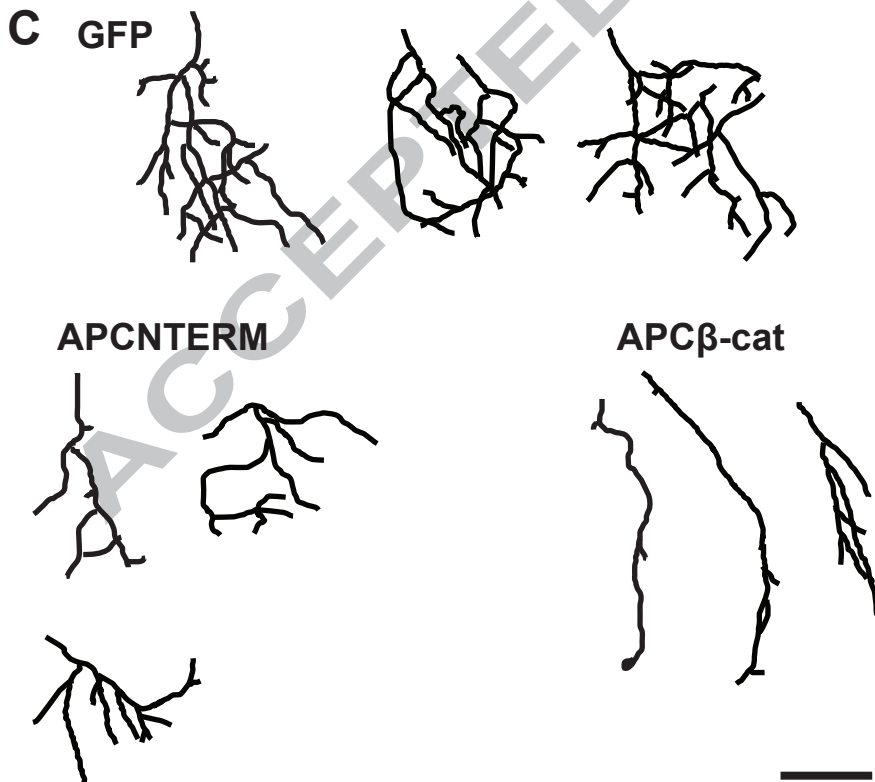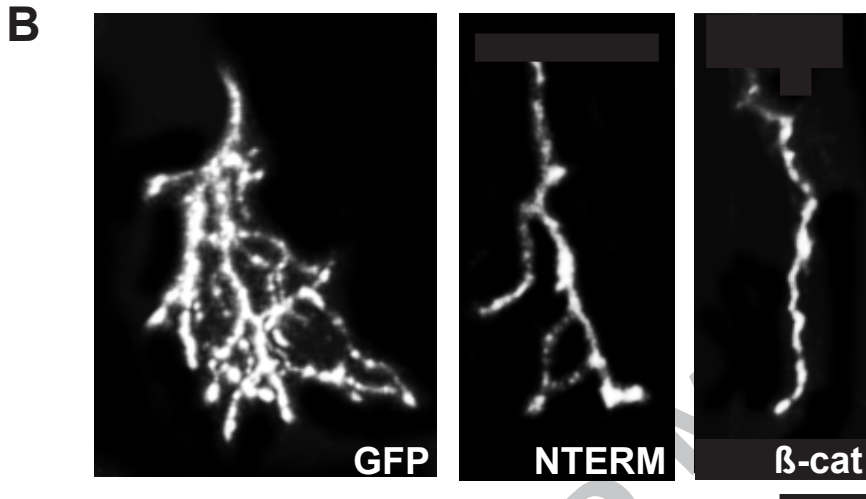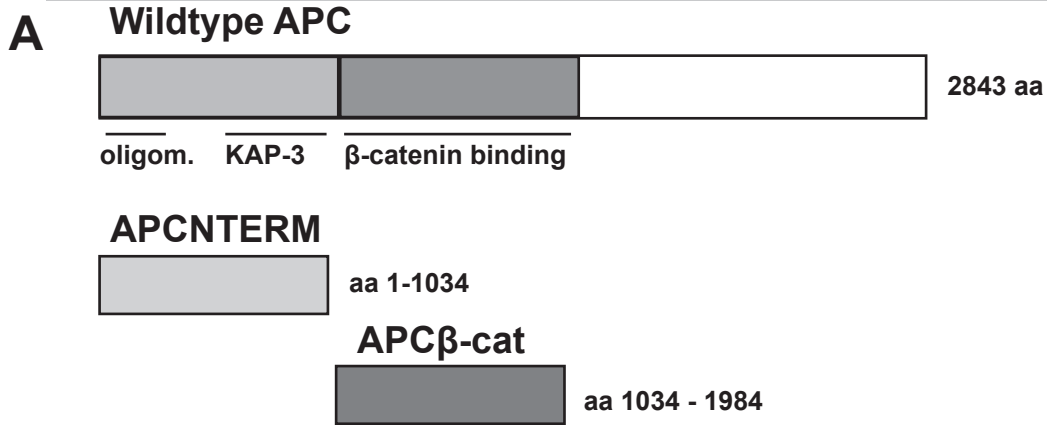
A **Wildtype APC**
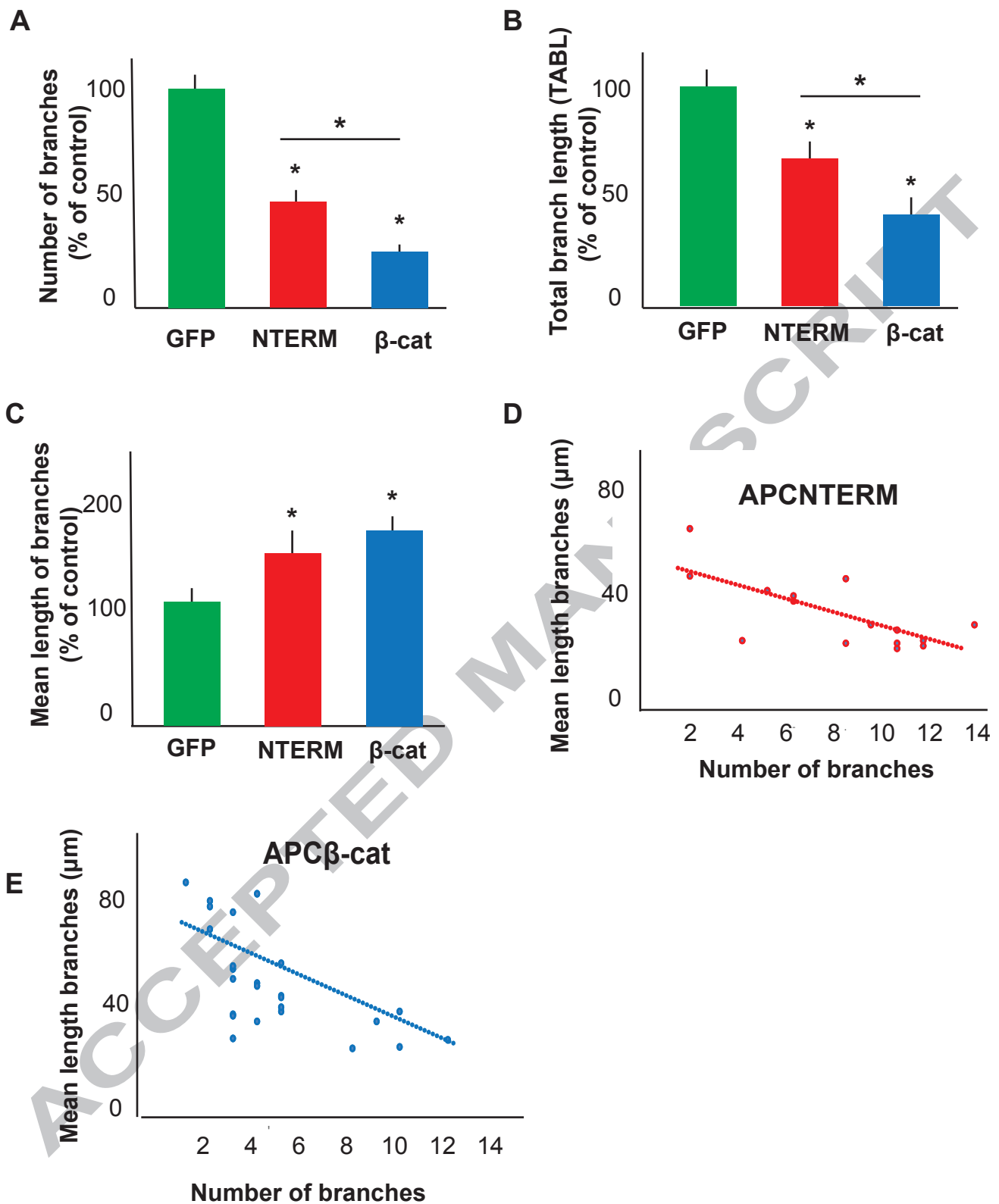
2843 aa

oligom.   KAP-3   β-catenin binding

APCNTERM

aa 1-1034

APCβ-cat

aa 1034 - 1984

B

GFP   NTERM   ß-cat

C   GFP

APCNTERM   APCβ-cat

Figure 1

Figure 2

A

GFP

APCNTERM APCβ-cat

B

$$\text{Mean angle} = \sum \alpha i / \sum i$$

C

GFP

Mean Angle = 66°

73 59

GFP

NTER

62

98

Mean Angle = 80°

NTER

β-cat

58

68

Mean Angle = 63°

β-cat

Figure 3

Figure 4